Measurements and Analysis of Dynamic Effects in the LARP Model Quadrupole HQ02b During Rapid Discharge

Massimo Sorbi, Giorgio Ambrosio, Hugo Bajas, Guram Chlachidze, Vittorio Marinozzi, Samuele Mariotto, and Gianluca Sabbi

***Abstract*—This paper presents the analysis of some quench tests addressed to study the dynamic effects in the 1-m-long 120-mm-aperture Nb_3Sn quadrupole magnet, i.e., HQ02b, designed, fabricated, and tested by the LHC Accelerator Research Program. The magnet has a short sample gradient of 205 T/m at 1.9 K and a peak field of 14.2 T. The test campaign has been performed at CERN in April 2014. In the specific tests, which were dedicated to the measurements of the dynamic inductance of the magnet during the rapid current discharge for a quench, the protection heaters were activated only in some windings, in order to obtain the measure of the resistive and inductive voltages separately. The analysis of the results confirms a very low value of the dynamic inductance at the beginning of the discharge, which later approaches the nominal value. Indications of dynamic inductance variation were already found from the analysis of current decay during quenches in the previous magnets HQ02a and HQ02a2; however, with this dedicated test of HQ02b, a quantitative measurement and assessment has been possible. An analytical model using interfilament coupling current influence for the inductance lowering has been implemented in the quench calculation code QLASA, and the comparison with experimental data is given. The agreement of the model with the experimental results is very good and allows predicting more accurately the critical parameters in quench analysis (MIITs, hot spot temperature) for the MQXF Nb_3Sn quadrupoles, which will be installed in the High Luminosity LHC.**

***Index Terms*—Niobium compounds, quench protection, superconducting accelerators.**

I. Introduction

THE High Gradient Quadrupole (HQ) magnet is developed within the LARP collaboration for the High Luminosity upgrade of the CERN Large Hadron Collider. The HQ magnet structure has been used in two different assemblies, HQ01 and HQ02 with two generations of Nb_3Sn coils [1], [2]. The HQ cross-section is shown in Fig. 1. In 2011–12, nine coils, C1–C9 were tested in the HQ01 magnet as reported in [3]–[5]. In 2013, four coils C15, 16, 17, 20 were tested in the HQ02 model [6]. The HQ02 conductor is made of 35-strand (RRP108/127) cable with a short sample current of 18.2 kA at 1.9 K (16.6 kA at 4.3 K) [7]. The HQ02 cable incorporated a 25-μm-thick, 8-mm-wide stainless steel core between the two layers of strands that significantly reduced the AC loss from inter-strand coupling currents [8].

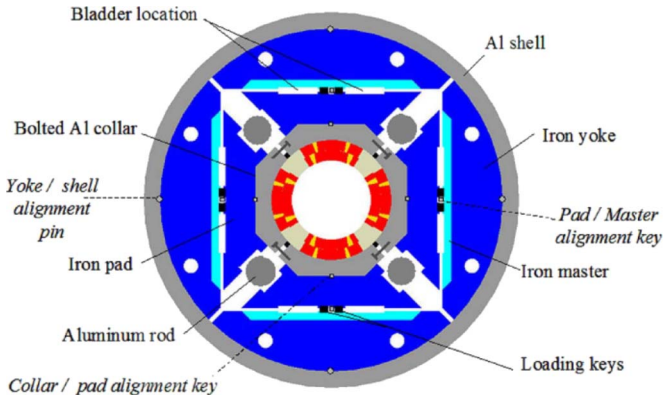

Fig. 1. High-gradient quadrupole (HQ) transverse cross section.

A first configuration of HQ02 was tested twice at Fermilab at temperatures ranging from 1.9 K to 4.5 K. These two tests refer to as HQ02a [6] and HQ02a2. In 2014, a second configuration, named HQ02b with a 15 MPa increase of azimuthal coil preload has then been tested at the CERN SM18 vertical test station at 1.9 K and 4.3 K. A general description of the test and of the results have been presented in [9]. In this paper, we analyze with more detail two of the last tests, that originally were intended to increase the accumulated MIITs (integration with respect to the time of the square current from the beginning of the transition) in the magnet during a quench. During these tests, both at 11 kA, quenches were provoked by firing a strip of the protection heater of one coil only (inner layer), and increasing the delay time that activates the rapid discharge on the dumping resistance and turning off of power supply; in this way the reduced speed of quench propagation (for a reduced value of the operating current), the low resistance of the quenched volume and the increased value of the delay time allowed to reach 14.7 MA^2s

Manuscript received October 20, 2015; accepted January 27, 2016. Date of publication February 3, 2016; date of current version February 16, 2016. This work was supported by the European Commission under the FP7 Project HiLumi LHC under Grant 284404 cofunded by the DoE, USA, and KEK, Japan.

M. Sorbi, V. Marinozzi, and S. Mariotto are with the Laboratorio Acceleratori e Superconduttività Applicata, Istituto Nazionale di Fisica Nucleare Sezione di Milano, 20090 Milan, Italy, and also with the University of Milan, 20090 Milan, Italy (e-mail: massimo.sorbi@mi.infn.it).

G. Ambrosio and G. Chlachidze are with the Fermi National Accelerator Laboratory, Batavia, IL 60510 USA.

H. Bajas is with the Technology Department, European Organization for Nuclear Research (CERN), 1211 Geneva, Switzerland.

G. Sabbi is with the Lawrence Berkeley National Laboratory, Berkeley, CA 94720 USA.

Color versions of one or more of the figures in this paper are available online at http://ieeexplore.ieee.org.

Digital Object Identifier 10.1109/TASC.2016.2524584

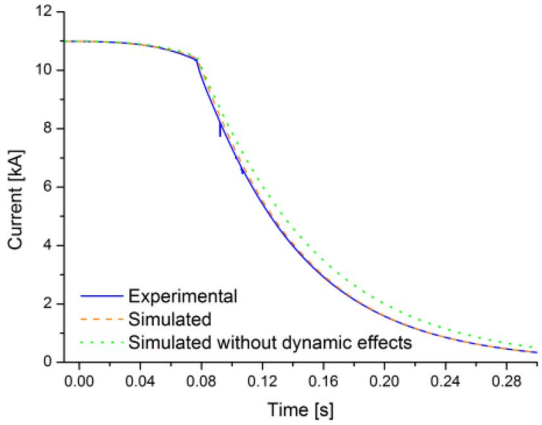

Fig. 2. Current versus time for quench test provoked in coil n. 16 and delay time of 80 ms. The picture reports also the current decay simulations, including and not including the dynamic effects for the inductance calculation (see Section III).

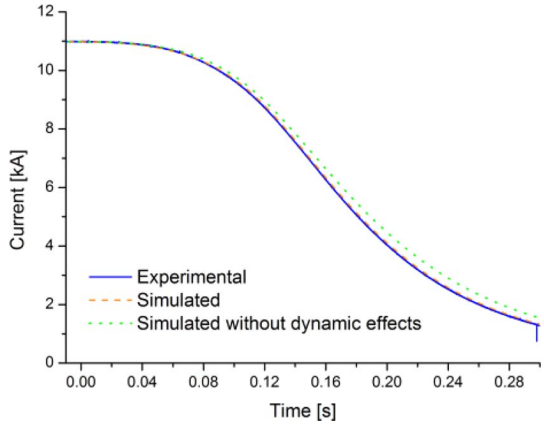

Fig. 3. Current versus time with quench provoked in coil n. 16 and delay time of 300 ms. The picture reports also the current decay simulations, including and not including the dynamic effects for the inductance calculation (see Section III).

and 19 MA^2s for the MIITs in the two tests. Beside this effect, another one was obtained: by firing the protection heater of one coil only, it was possible to detect directly the inductive and resistive voltages during the beginning of the transition; in fact because the quench starts not in all the four coils, the voltages of the not quenched coils can be assumed to be purely inductive; considering that the four coils are identical, it is then possible to obtain a direct measurement of the inductance of the whole magnet during the quench. Other measurements on magnets have showed indeed that the inductance at the beginning of a transition assumes different values with respect to the measured value in "static" condition, i.e., with slow current ramp rate [10], [11]. In fact during a transition the rapid change of the current induces eddy currents on the conductor and on the other metallic parts of the magnet which sensibly decrease the apparent inductance of the coils ("dynamic effect"). In [10], [11] the dynamic effect in superconducting quadrupole during rapid discharge for quench have been presented, and a model to describe this phenomenon by considering the magnetization of the conductor for the large value of the inter-filament coupling currents (IFCC) has been presented. Here, we apply the same model to the HQ02b measurements and we presents the results.

II. Inductance Measurements During a Quench

In this section we report the analysis of the experimental data from the two tests of HQ02b in order to obtain a direct measurement of the inductance during the quench. The experimental data from the acquisition system were the currents vs. time and the voltages of each of the 4 coils (named coil number 15, 16, 17, and 20) vs. time, which have been acquired with a frequency of 100 kHz. Figs. 2 and 3 report the graphs of current vs. time of the two considered test: the first one had a delay time of 80 ms before the activation of the discharge on the dumping resistance of 60 mΩ (actually in [9] the delay and the resistance were reported as 110 ms and 40 mΩ, but it has to be an error, as it can be easily verified with Fig. 2) and the other one had a delay of 300 ms. The analysis includes the first 300 ms, so for the first test there is also the discharge in the dumping resistor, whereas for the second one it stops just before.

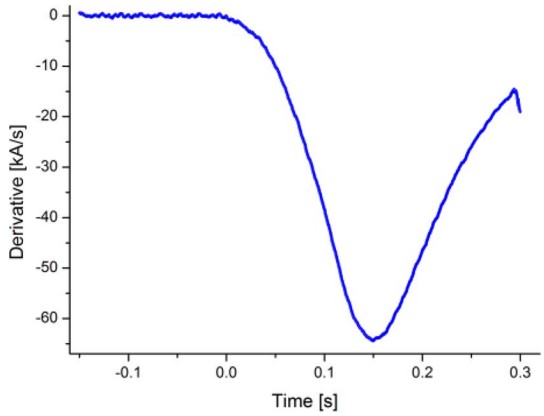

Fig. 4. Current derivative versus time with quench provoked in coil n. 16 and delay time of 300 ms, calculated numerically and smoothed.

The current derivative can be calculated numerically from this data, but it requires a smoothing process, because the noise completely masks the calculated signal. Fig. 4 reports the graph of the current derivative, numerically calculated and smoothed applying twice a moving average 3.5 ms wide, which resulted the best compromise to obtain clean signal keeping a temporal resolution of the order of 10 ms [12].

It was necessary to apply a smoothing process to the voltages signal too, in order to suppress the noises. The Fig. 5 reports the graph of the coil 17 voltage vs. time just before and at the beginning of the quench provoked in coil 16. After a first smoothing with a moving average of 3.5 ms, the signal is enough clean but a typical 50 Hz noise from the grid power is still present (Fig. 6). We proceeded to suppress it by subtracting an equivalent 50 Hz sinusoidal signal with the same phase which was fitted from the voltage curve (red curve in Fig. 6).

The voltages across each coil in the magnet, after the smoothing and 50 Hz noise suppression, is represented in Figs. 7 and 8 for the two quenches. Coil 17 and coil 20 voltages assume very similar values; coil 16 has the largest value because it is the one where the quench was initially provoked, whereas coil 15 assumes an intermediate value. From these data it is the possible

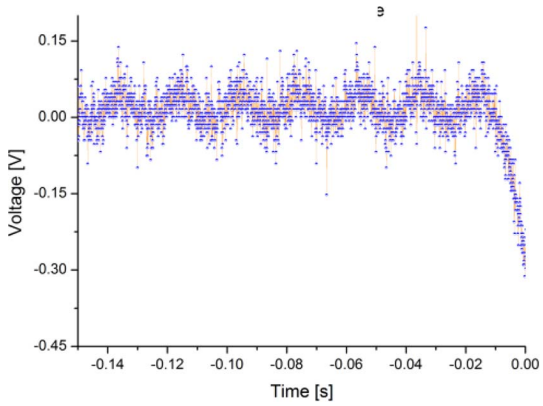

Fig. 5. Voltage versus time of coil 17 just before and at the beginning of quench provoked in coil 16: raw signal.

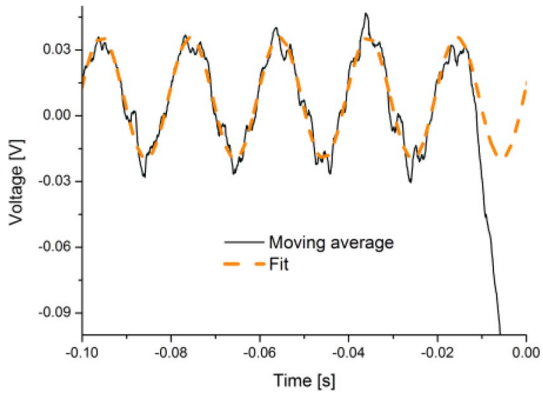

Fig. 6. Voltage versus time of coil 17 after a first smoothing with average moving. The 50-Hz noise superimposed to the signal is evident, which can be fitted (red curve) and then subtracted.

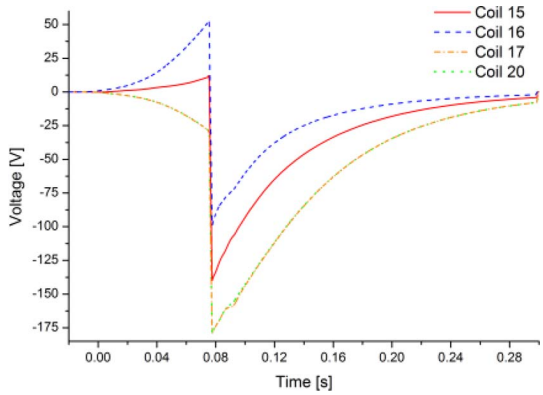

Fig. 7. Voltages versus time on each coil after smoothing and 50-Hz noise suppression with quench provoked in coil n. 16 and delay time of 80 ms.

to infer that initially coil 17 and 20 do not quench: they have the same inductive signal, and two perfect symmetric spontaneous quenches in both coils is so unlikely to not be considered (actually they do quench for quench back after about 90 ms, as described in Section III, and in fact their voltage signals in Fig. 8 start to differ after 90 ms). Coil 15 is affected by a quench, probably propagated from coil 16 through the cable connection.

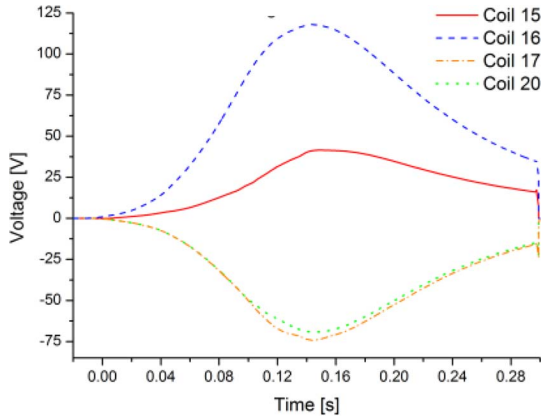

Fig. 8. Voltages versus time on each coil after smoothing and 50-Hz noise suppression with quench provoked in coil n. 16 and delay time of 300 ms.

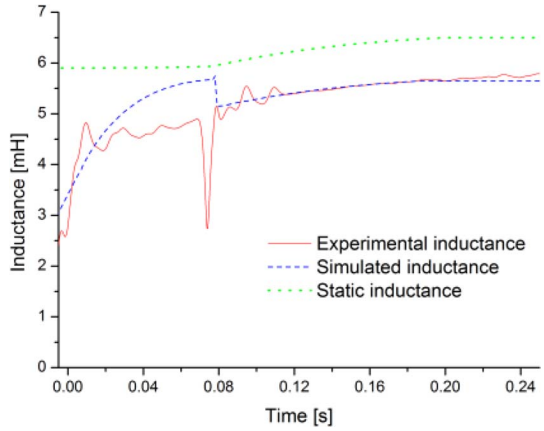

Fig. 9. Experimental inductance versus time for quench test provoked in coil n. 16 and delay time of 80 ms. The picture reports also the simulated dynamic inductance (see Section III). The variation of the simulated static inductance after t = 0.08 s is due to the iron yoke desaturation during the discharge.

Calling V_{17} the smoothed voltage across coil 17 (or across coil 20), the total inductance L_d of the magnet can be evaluated as:

$$L_d = 4 \cdot V_{17} / \frac{dI}{dt}. \tag{1}$$

The Figs. 9 and 10 report the behavior of L_d for the two considered quenches.

Despite the careful smoothing process of the signals of voltages and of current derivate, the "experimental inductance" curves still present some anomalous oscillations, which can give an indication of the amplitude of the error of its evaluation. The rapid oscillation of L_d at about 90–100 ms for the case with "80 ms delay" in Fig. 9 is due to the opening of the main switch and to the discharge of the current in the dumping resistance. Both measurements of the inductance L_d are below the nominal value in "static condition"; at the beginning of the quench L_d assume much lower values, and then it increases in about 10 ms. These difference of the inductance L_d with respect to nominal value measured in "static condition" can be interpreted as dynamic effects for the large and rapid variation of the magnetic field during the quench.

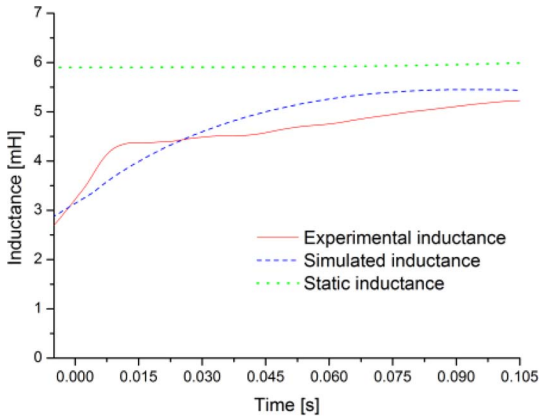

Fig. 10. Experimental inductance versus time for quench test provoked in coil n. 16 and delay time of 300 ms. The picture reports also the simulated dynamic/static inductances (see Section III). The graph is intentionally interrupted at 100 ms because the "experimental inductance" given by (1) is meaningless when back quenches start in coil 17 and 20 at about 90 ms (see Section III for details).

III. Simulation of Quench With Dynamic Effects

A detailed model to describe the variation of the superconducting magnet inductance during the rapid discharge following a provoked quench has been presented in [10], [11]. In that model the effect of IFCC was considered and the equivalent magnetization of the coil is considered; the IFCC have their own time constant τ:

$$\tau = \frac{\mu_0}{2\rho_{et}} \left(\frac{L}{2\pi} \right)^2 \tag{2}$$

which depends on the strand characteristics (twist pitch L and effective transverse resistivity ρ_{et}) [13]; the IFCC are induced by the transport current in the magnet which decays for the quench. As results, the equivalent magnetization in the coil region continues to vary, giving a non-negligible contribution for the magnetic energy U of the magnet. From the magnetic energy of the magnet is then possible to calculate the true dynamic inductance L_d as:

$$L_d = \frac{d\phi}{dI} = \frac{1}{I} \frac{dU}{dI} \tag{3}$$

According to this model, the dynamic inductance L_d varies during the discharge and is lower than the static inductance value due to the contribution of the magnetization M in the magnetic energy U.

This method to evaluate the dynamic inductance in superconducting magnet has been implemented in the quench code QLASA [14], which now simulates the quench evolution and the discharge of the magnet taking into account also the inductance variation from the IFCC. The results are presented in Figs. 2 and 3, where the current discharge is plotted and compared with the simulations. In the graph also a simulation not-including the dynamic effects has been included, in order to show how this effect is necessary to reproduce the behavior of the current decay. The time constant τ which best reproduces the experimental data is 30 ms, to be compared with a theoretical value of about 10–15 ms based on the nominal twist pitch

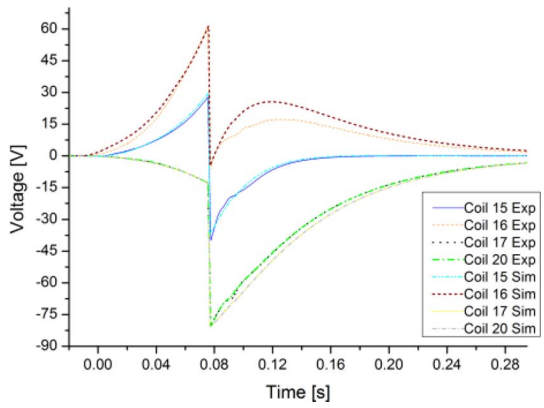

Fig. 11. Experimental and simulated voltages on inner layers of each coil (quench provoked in coil n. 16 and delay time of 80 ms).

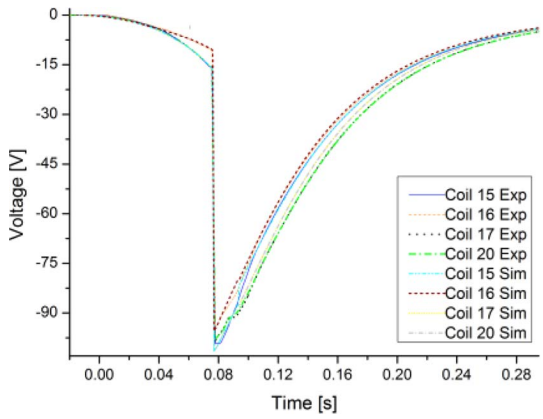

Fig. 12. Experimental and simulated voltages on outer layers of each coil (quench provoked in coil n. 16 and delay time of 80 ms).

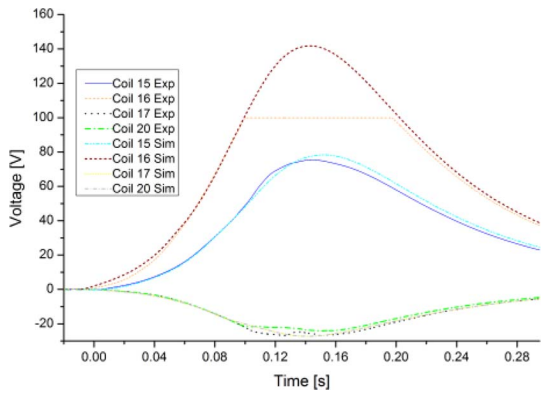

Fig. 13. Experimental and simulated voltages on inner layers of each coil (quench provoked in coil n. 16 and delay time of 300 ms).

L and effective transverse resistivity ρ_{et}. In Figs. 11–14 the experimental and simulated value of the voltages in the inner and outer layers for each coil are reported; the agreement is overall quite good. To fit the curves, a quench back also in coil 17 and coil 20 has been initiated in the simulation with a delay of about 90 ms.

The acquisition of purely inductive voltage signal for coil 17 and 20 allowed to obtain the experimental resistive voltage of

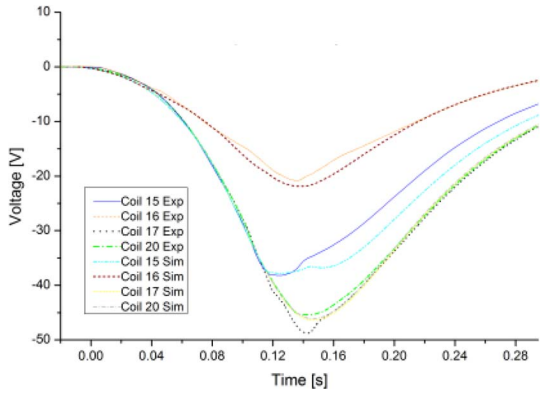

Fig. 14. Experimental and simulated voltages on outer layers of each coil (quench provoked in coil n. 16 and delay time of 300 ms).

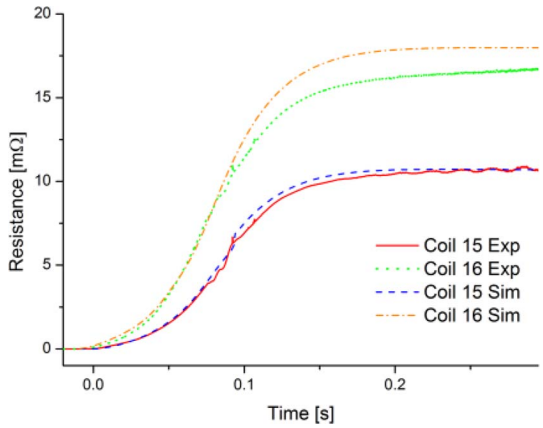

Fig. 15. Experimental and simulated resistance of coil 15 and 16 (quench provoked in coil n. 16 and delay time of 80 ms).

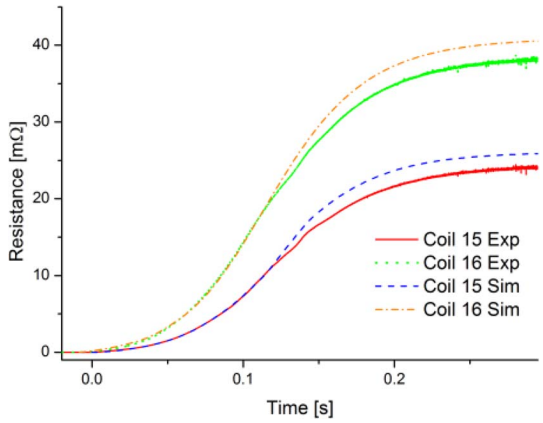

Fig. 16. Experimental and simulated resistance of coil 15 and 16 (quench provoked in coil n. 16 and delay time of 300 ms).

the coil 15 and 16 (difference between total voltage in coil 15 and 16 and inductive voltages). The Figs. 15 and 16 report the comparison of the so obtained "experimental" resistances in coil 15 and 16 with respect to simulated. The agreement is very good up to about 100 ms; later the difference increases because the experimental resistance is under-estimated: in fact in the subtraction the growing resistive voltage of coil 17 and 20 (which have a quench back at about 90 ms) is not properly accounted for.

IV. Conclusion

An experimental study of the dynamic inductance in superconducting magnets during a quench has been presented. A direct measurement of its value was possible starting from the inductive voltage signal of the non-quenching coils. As expected, the dynamic inductance during rapid discharge results considerable lower than the inductance in static condition, especially at the beginning of the quench. The model to calculate this variation of inductance for the coupling of IFCC, implemented in the quench code QLASA, has been compared with the experimental data (current and partial voltages across the coils). The general agreement is very good, showing that the right description of the dynamic inductance is necessary to reproduce correctly the experimental data. The validation of the model allows to use it for more precise quench studies of high field, high energy density superconducting magnets, where the decrease of the magnet inductance during the discharge for dynamic effects may play a significant role to contain the hot spot temperature.

References

[1] G. Sabbi, "Nb_3Sn IR quadrupoles for the high luminosity LHC," *IEEE Trans. Appl. Supercond.*, vol. 23, no. 3, Jun. 2013, Art. ID 4000707.

[2] S. Caspi *et al.*, "Design of a 120 mm bore 15 T quadrupole for the LHC upgrade phase II," *IEEE Trans. Appl. Supercond.*, vol. 20, no. 3, pp. 144–147, Jun. 2010.

[3] P. Ferracin *et al.*, "Mechanical behavior of HQ01, an Nb_3Sn accelerator quality quadrupole magnet for the LHC luminosity upgrade," *IEEE Trans. Appl. Supercond.*, vol. 22, no. 3, Jun. 2012, Art. ID 4901804.

[4] M. Marchevsky *et al.*, "Quench performance OF HQ01, a 120 mm bore LARP quadrupole for the LHC upgrade," *IEEE Trans. Appl. Supercond.*, vol. 22, no. 3, Jun. 2012, Art. ID 4702005.

[5] H. Bajas *et al.*, "Cold test results of the LARP HQ Nb_3Sn quadrupole magnet at 1.9 K," *IEEE Trans. Appl. Supercond.*, vol. 23, no. 3, Jun. 2013, Art. ID 4002606.

[6] G. Chlachidze *et al.*, "Performance of HQ02, an optimized version of the 120 mm Nb_3Sn LARP quadrupole," *IEEE Trans. Appl. Supercond.*, vol. 24, no. 3, Jun. 2014, Art. ID 4003805.

[7] A. Godekeetal, "A review of conductor performance for the LARP high gradient quadrupole magnets," *Supercond. Sci. Technol.*, vol. 26, no. 9, Aug. 2013, Art. ID 095015.

[8] X. Wang *et al.*, "Multipoles induced by inter-strand coupling currents in LARP Nb_3Sn quadrupoles," *IEEE Trans. Appl. Supercond.*, vol. 24, no. 3, Jun. 2014, Art. ID 4002607.

[9] H. Bajas *et al.*, "Test results of the LARP HQ02b magnet at 1.9 K," *IEEE Trans. Appl. Supercond.*, vol. 25, no. 3, Jun. 2015, Art. ID 4003306.

[10] V. Marinozzi *et al.*, "Study of quench protection for the Nb_3Sn low-β quadrupole for the LHC luminosity upgrade (HiLumi-LHC)," *IEEE Trans. Appl. Supercond.*, vol. 25, no. 3, Jun. 2015, Art. ID 4002905

[11] V. Marinozzi *et al.*, "Effect of coupling currents on the dynamic inductance during fast transient in superconducting magnets," *Phys. Rev. ST—Accel. Beams*, vol. 18, no. 3, Mar. 2015, Art. ID 032401.

[12] S. Mariotto, "Studio e analisi della propagazione del quench in un quadrupolo superconduttivo ad alto campo magnetico in presenza di effetti dinamici," Laurea thesis, Dept. Phys., Univ. Studi Milano, Milano, Italy, 2014

[13] M. N. Wilson, *Superconducting Magnets*. Oxford, U.K.: Clarendon, 1983.

[14] L. Rossi and M. Sorbi, "QLASA: A computer code for quench simulation in adiabatic multicoil superconducting windings," Nat. Inst. Nucl. Phys., Rome, Italy, Tech. Rep. TC-04-13, 2004.